Electronic Supplementary Material (ESI) for RSC Advances.
This journal is © The Royal Society of Chemistry 2016

Supporting Information

Title: **High performance ionic and non-ionic fluoropolymer/ionic liquid gel hybrid actuators based on single-walled carbon nanotubes**

Authors: **Naohiro Terasawa***

Affiliation:

Inorganic Functional Material Research Institute, National Institute of Advanced Industrial Science and Technology (AIST), 1-8-31 Midorigaoka, Ikeda, Osaka 563-8577 Japan

Table S1 Comparison of the values of electrical conductivity (**S·cm^{-1}**) of various polymer gel electrode layers containing an IL (EMI[BF_4] or EMI[TFSI]).

Electrode	BF_4	TFSI
PVdF(HFP)/Nafion = 1:1	19.9	24.4
PVdF(HFP)/Nafion = 1:3	22.8	24.9
PVdF(HFP)	17.5	16.0

Table S2 Comparison of the self-diffusion coefficients of cations $\boldsymbol{D}_+$ (10^{-7} cm^2·s^{-1}) and anions ***D-*** (10^{-7} cm^2·s^{-1}) in pure samples of ILs. (Data are taken from Refs. S1 and S2.)

IL	D_+	D-
EMI[TFSI]	6.2	3.7
EMI[BF_4]	4.9	3.9

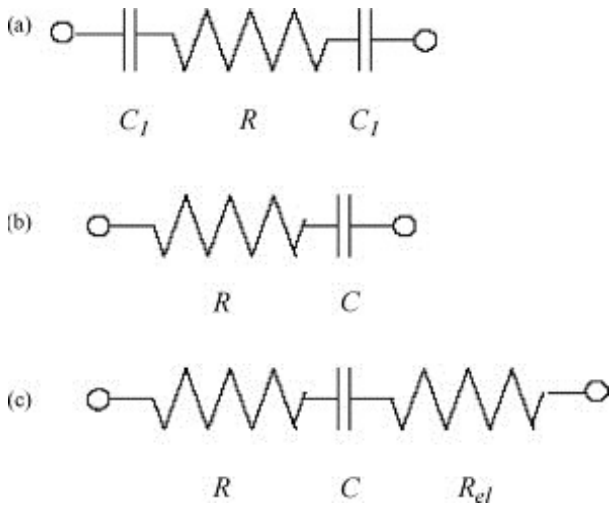

Figure S1 Equivalent circuit models of the bucky-gel actuator. (a) Model consisting of specific capacitance C_1 and ionic resistance R. (b) Model in which the specific capacitance is represented by $C = C_{1/2}$. (c) Model consisting of specific capacitance C, ionic resistance R, and electrode resistance R_{el}.

Figure S1 shows the equivalent circuit models for the Nafion™–PVdF(HFP)–SWCNT–IL actuators. The model shown in Fig. S1(a) consists of specific capacitance C_1 between the Nafion™–PVdF(HFP)–SWCNT–IL electrode and the electrolyte layer and resistance R, which is associated with the electrolyte layer. Fig. S1(b) shows a more simplified model in which the two C_1 capacitances are replaced by single capacitance C (= $C_1/2$). When a triangular voltage with an amplitude of $\pm A$ and frequency of f is applied to the equivalent circuit shown in Fig. S1(b), the maximum accumulated charge $Q(f)$ can be expressed as follows [S3]:

$$Q(f)/Q_0 = 1 - 4CRf\,(1 - \exp(-1/4CRf)), \tag{S1}$$

where Q_0 is the accumulated charge in the low-frequency limit. If strain ε in the electrode layer is proportional to the accumulated charge, it can be calculated as follows:

$$\varepsilon = \varepsilon_0\, Q(f)/Q_0, \tag{S2}$$

where ε_0 is the strain in the low-frequency limit.

When conduction in the electrode layer is considered, the electrode resistance must be accounted for in the equivalent circuit. If the electrode resistance is explicitly treated, the

equivalent circuit should be treated as a distributed transmission line [S4]. Here, we assumed that the electrode resistance consists of resistance element R_{el}, as shown in Fig. S1(c); thus, R in Eq. (S1) can be replaced by $R + R_{el}$.

To evaluate the double-layered charging kinetic model, the specific capacitance of the Nafion™– PVdF(HFP)–SWCNT–IL electrode and the ionic resistance of the gel electrolyte layer were measured. The frequency dependence of the strain was calculated using Eqs. (S1) and (S2). Fig. 5 shows the frequency dependence of the measured strain values, together with the simulation results of the Nafion™–PVdF(HFP)–SWCNT–EMI[BF_4] device with PVdF(HFP):Nafion™ ratio = 1:3. Curve A was calculated using the model shown in Fig. S1(b), and Table S3 lists the simulation parameters. Curve B was calculated using the model shown in Fig. S1(c); the corresponding simulation parameters are listed in Table S4. Surprisingly, in contrast to the PVdF(HFP)–SWCNT–IL device [S3], Fig. 5 clearly shows that the frequency dependence of the strain is well reproduced by Curve A. Furthermore, Fig. 5 clearly shows that the frequency dependence of the strain is reproduced by the double-layered charging kinetic model when we consider only the electrolyte resistance. Similar results were obtained for the Nafion™–PVdF(HFP)–SWCNT–EMI[TFSI] device with PVdF(HFP):Nafion™ ratio = 1:3 and Nafion™–PVdF(HFP)–SWCNT–IL device with PVdF(HFP):Nafion™ ratio = 1:1. To fit the strain values in the low-frequency limit in Fig. 5, appropriate values were chosen for ε_0 in Eq. (S1); these values are listed in Table S3.

Table S3 Simulation parameters for the model that ignores the electrode resistance.

IL	C_{SWCNT} (F g^{-1})	C (F cm^{-2})	κ (mS cm^{-1})	R (Ω cm^2)	ε_0 (%)	CR (s)
EMI[BF_4]	116.6	0.198	0.66	3.03	0.54	0.599
EMI[TFSI]	63.9	0.114	0.41	4.88	0.40	0.556

Table S4 Simulation parameters for the model that considers the electrode resistance.

IL	C (F cm^{-2})	R_{el}(Ω cm^2)	$R+R_{el}$ (Ω cm^2)	$C(R+R_{el})$ (s)
EMI[BF_4]	0.198	7.31	10.34	2.047
EMI[TFSI]	0.114	6.69	11.57	1.319

R_{el} = area of the electrode film (**cm^2**)/[(electrical conductivity (**S·cm^{-1}**) × thickness of the electrode film (**cm**)] [S3].

Table S5 Comparison of the Young's moduli (**MPa**) of different electrodes.

Electrode	BF_4	TFSI
PVdF(HFP)/Nafion=1:1	142	122
PVdF(HFP)/Nafion=1:3	143	120
PVdF(HFP)	175	132

References

[S1] H. Tokuda, S. Tsuzuki, Md. A.B.H. Susan, K. Hayamizu, M. Watanabe, J. Phys. Chem. B, 110 (2006) 19593−19600.

[S2] S. Tsuzuki, T. Umecky, H. Matsumoto, W. Shinoda, M. Mikami, J. Phys. Chem. B, 114 (2010) 11390–11396.

[S3] I. Takeuchi, K. Asaka, K. Kiyohara, T. Sugino, K. Mukai, T. Fukushima**,** T. Aida, Electrochim. Acta, 53 (2009) 1762–1768.

[S4] K. Takagi, Y Nakabo, Z.-W. Luo, K. Asaka, Proceedings of the SPIE, Electroactive Polymer Actuator and Devices (EAPAD), 6524 (2007) 652416-1–652416-8.